

Redesign of the Coils for the 60T Controlled-Waveform Magnet at NHMFL

Doan N. Nguyen, Do T. Vo, James R. Michel , Iain Dixon , Todd Akins, and Ke Han 

Abstract—Driven by the 1.4 GW generator, the 60T Controlled-Waveform (60 TCW) magnet was the most powerful controlled waveform system in the world and had always been one of most important magnets to the National High Magnetic Field (NHMFL) and high-field research community because of its following unique features: (1) quasi-static field up to 60 T with 100 ms flat-top and total pulse-length of about 2000 ms, (2) variable magnetic field waveforms such as staircase and triangle with flat-top (3) relative large bore (32 mm) and (4) very fast cooling time (20 minutes) between pulses [Boebinger, 2001], [Crooker *et al.* 2001]. The magnet is composed of nine concentric coils, with each coil consisting of several conductor winding layers reinforced by a high-strength metallic shell. The magnet underwent a catastrophic failure in 2000 and all the coils had to be rebuilt. In late 2014 the second magnet version failed near the mid-plane of coil 7. The simulations afterward that incident indicated that the overall strength of the coil would be increased by replacing a section of the reinforcing shell with Zylon fiber-epoxy composite. This reduces the stress and thus significantly lowers the level of plastic deformation in the windings. The role of the metal and Zylon fiber reinforcing layers in bearing the axial and radial Lorentz forces has been studied to optimize the magnet design. The results of the optimization will be discussed as well as challenges that have been presented in rebuilding the individual coils of the magnet.

Index Terms—High magnetic field, magnet design, pulsed magnet.

I. INTRODUCTION

THE UNIQUE 60TCW magnet of the Pulsed Field Facility (PFF) – NHMFL at Los Alamos consists of nine concentric coils as seen in Fig. 1. The coils were designed with the same concept, each composes of several conductor layers reinforced by a metallic shell. The hoop stress in coil winding is proportional to the radial Lorentz forces acting on the winding and the radius of the winding. Thus, out of the nine coils of our 60TCW magnet, coils 1, 2, 8 and 9 (two innermost and two outermost coils) experience lower hoop stress than the other coils do. So these coils were wound with Glidcop AL15 which has the room temperature ultimate tensile strength (UTS) of about 480



Fig. 1. Photograph of 9 magnet coils of the 60TCW magnet.

TABLE I
WINDING SPECIFICATION FOR THE MAGNET COILS

Coil #	# of layers	Material	Total length (m)	Conductor size (mm ²)	Shell material
Coil 1	2	AL15	4.5	4.3 x 9.2	Ni40
Coil 2	2	AL15	12.5	4.3 x 9.2	Ni40
Coil 3	2	AL60	31.5	5.2 x 8.6	Ni40
Coil 4	2	AL60	59	5.2 x 8.6	Ni40
Coil 5	4	AL60	223.5	5.2 x 8.6	Ni40
Coil 6	4	AL60	385	6.7 x 11	Ni40
Coil 7	6	AL60	785	6.7 x 11	Ni40
Coil 8	6	AL15	910	7.5 x 12.5	Ni40
Coil 9	6	AL15	1120	7.5 x 12.5	SS301

MPa. Coils 3 to 7 experience higher hoop stress and therefore were wound with stronger wire, Glidcop AL60, of which room temperature UTS is about 580 MPa. Coils 1 to 8 use forged Nitronic 40 (Ni40) shells as the reinforcements while low-stress coil 9 uses a roll formed stainless steel reinforcing shell. Table I summarizes the design and materials used in the all nine coils of the magnet. That magnet design was aimed to deliver a level of about 10000 full-field (60T) pulses.

The magnet was first brought online in 1997, but it experienced a catastrophic failure in 2000 with magnet lifetime much shorter than expected [4], [5]. Autopsying failed coils indicated that the incident was caused by a brittle sigma phase inside the reinforcing Ni40 shells [6], [7]. It took PFF nearly 6 years to requalify the fabrication processes for the Ni40 shells and rebuild the second version of magnet coils (named 60TCW magnet Mark II) [8], [9].

The nine coils were grouped into three coil-groups which are powered by independent power-supplies: Group consists of coils 1 to 5; group 2 consists of coils 6 and 7, and group 3 consists of

Manuscript received November 29, 2021; revised January 16, 2022; accepted February 1, 2022. Date of publication February 23, 2022; date of current version March 11, 2022. This work was supported in part by Pulsed Field Facility (NHMFL), Los Alamos National Laboratory and PFF, and in part by NSF under Grants DMR-1157490 and DOE. (Corresponding author: Doan N. Nguyen.)

Doan N. Nguyen, Do T. Vo, and James R. Michel are with Los Alamos National Laboratory, Los Alamos, NM 87544 USA (e-mail: doan@lanl.gov).

Iain Dixon, Todd Akins, and Ke Han are with National High Magnetic Field Laboratory, Tallahassee, FL 32310 USA.

Color versions of one or more figures in this article are available at <https://doi.org/10.1109/TASC.2022.3151836>.

Digital Object Identifier 10.1109/TASC.2022.3151836

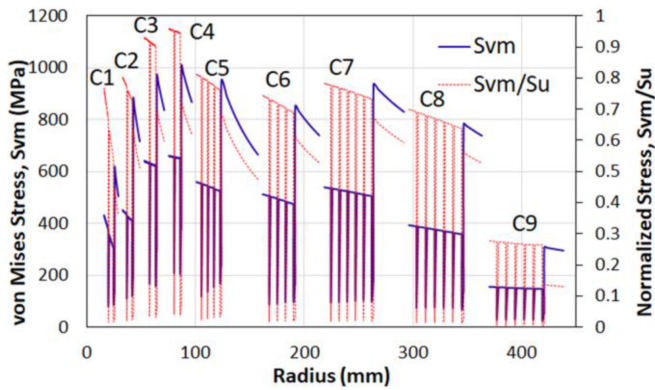


Fig. 2. Mid-plane von Mises stress, S_{vm} (solid line) and its ratio to the UTS of corresponding materials, S_{vm}/S_u (dashed line) for all nine coils.

coils 8 and 9. The magnet was purposely designed to have the stress in coils of group 1 slightly higher than in coils of group 2 because group 1 stores lower magnetic energy than group 2 does. The design was not very well optimized as the stresses were not equal for individual coils of each coil-group. Fig. 2 depicts the mechanical performance of the magnet coils of the Mark II at the peak field of 60T. The solid blue line is the von Mises stress and the dashed red line is the von Mises stress normalized to the UTS of the corresponding materials. For coil-group 1, stress in coils 3 and 4 higher than that of other coils. For coil-group 2, stress in coil 7 is higher than that in coil 6. The Mark II experienced a soft failure in coil 7 in December 2014 [9]. PFF has been working on redesigning and rebuilding the coils 3, 4 and 7 for the magnets [10].

II. REDESIGNING COILS OF THE MAGNET

A. Redesigning Requirement and Approach

After the second failure, inspections indicated that coil 3, 4 and 7 need to be rebuilt and the other coils are still in good shape and can be reused. Also, all the lead and supporting structures will be reused to save the cost. Thus, all the rebuilt coils should have exactly the same dimensions and winding specification as the old coils. We propose to replace a part of Ni40 metal shells of the rebuilt coils with Zylon fiber which has a Young's modulus of 265 GPa and ultimate tensile strength of about 5 GPa, considerably higher than those of Ni40 alloy [11], [12]. We expect that high-modulus, high-strength Zylon fiber will take more hoop load and reduce the stress in the windings. To maintain the dimensions, the Ni40 shells were cut with a pocket and Zylon fiber will be installed into that pocket to ensure the coil outer diameters are unchanged (see Fig. 3).

While having exceptionally high tensile strength for the hoop load, Zylon fiber composite has a low shear strength to handle the axial stress. It is critical to optimize the depth of the pocket to reasonably bear for both hoop and axial stresses. Our calculations indicated that Zylon fiber composite can be used to replace 35% of the Ni40 shell thickness for coils 3 and 4 and 30% of the thickness of the Ni40 shell of coil 7.

B. Mechanical Performance of Redesigned Coils

Fig. 4 illustrates the calculated von Mises stress distribution for a quarter of the cross-section of the magnet with the new

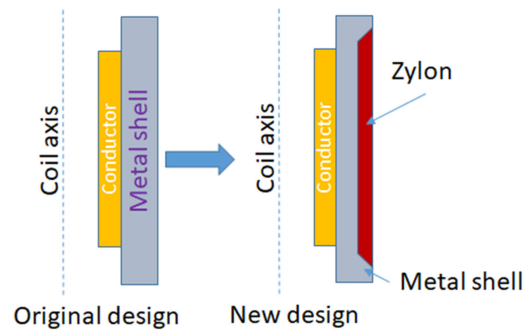


Fig. 3. Illustration of how a part of a Ni40 metal shell is replaced by Zylon composite.

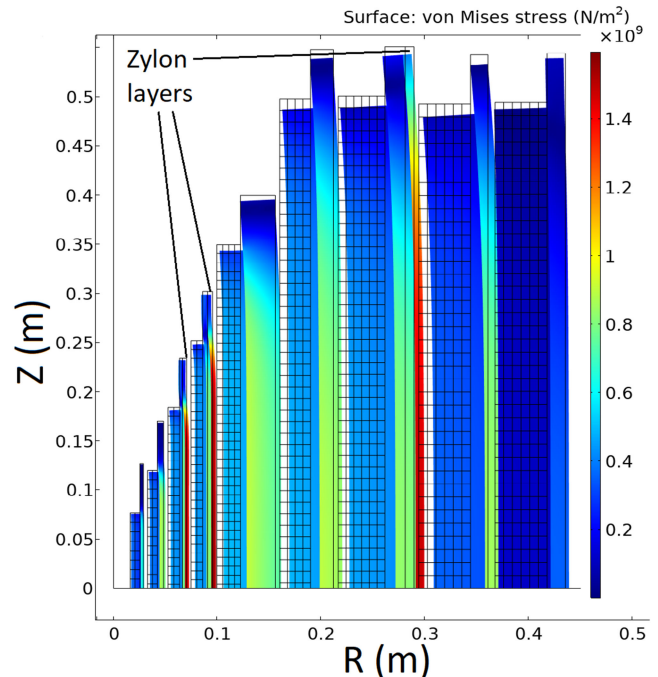


Fig. 4. von Mises stress distribution for a quarter of cross-section of the redesigned magnet at 60T field.

design at 60T field. As seen in the figure, the Zylon fiber composite layers in coils 3, 4 and 7 take a significant amount of the hoop load and the von Mises stress in those layers approaches 1500 MPa. The stress in the conductor winding is considerably reduced as seen in Fig. 5 which plots the mid-plane von Mises stress normalized to the UTS (S_{vm}/S_u) for all nine coils. With the new design, the von Mises stress in the windings of coils 3 and 4 is reduced to about 0.82 of the UTS of the AL60 conductor, nearly same as the stress level in coil 5. The von Mises stress in the windings of coil 7 is reduced from ~ 0.78 to 0.77 of the UTS of the AL60 conductor. With a thick winding in this coil, the improvement of stress in the innermost winding layer by adding Zylon seem to be not as much as we saw in coils 3 and 4. However, the stress level, $S_{vm}/S_u = 0.77$ in coil 7 is acceptable as it is still quite lower than that in coil 3 and 4.

The high stress in coils 3 and 4 of the old design caused considerably permanent deformation in those coils. The old coil 4 experienced the highest stress, therefore, it experienced the largest permanent deformation. Fig. 6 plots the permanent radial displacement of the coil 4 along the coil, as measured when

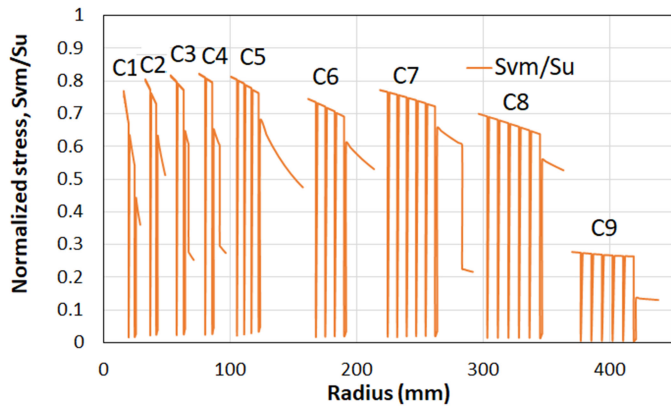


Fig. 5. Mid-plane von Mises stress normalized to the UTS of the corresponding materials for all the coils of the redesigned magnet at 60T field.

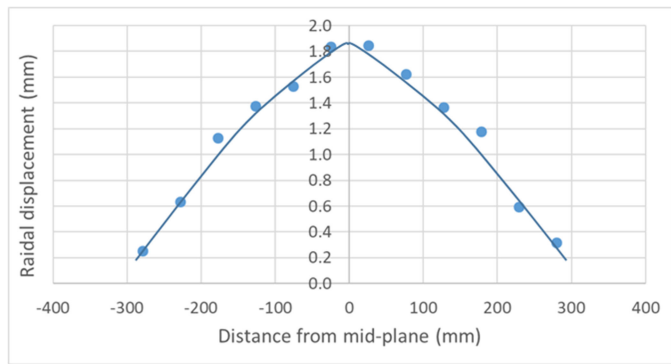


Fig. 6. Permanent radial displacement of the coil 4 along the coil. Measurements were carried out after the failure in 2014.

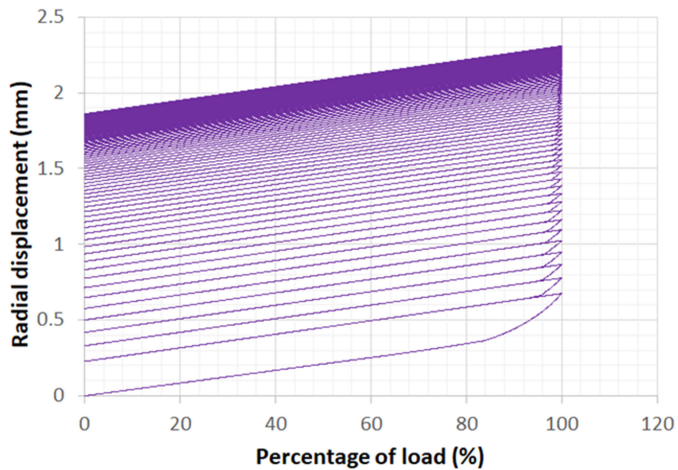


Fig. 7. Calculated radial displacement in the mid-plane of the coil 4 with the old design during 195 cycles of full-field 60T pulses.

we inspected it after the failure in 2014. The deformation is largest in the mid-plane reaching about 1.9 mm radially. The deformation near the winding end is much lower, as expected. Based on the fatigue stress-strain curves measured on AL60 conductor and reinforcing materials, we simulated the radial deformation (displacement) of coil 4 at its mid-plane. Figs. 7 and 8 describe the radial displacement after 195 full-field pulses of 60 T for the old and the new designs, respectively. At no

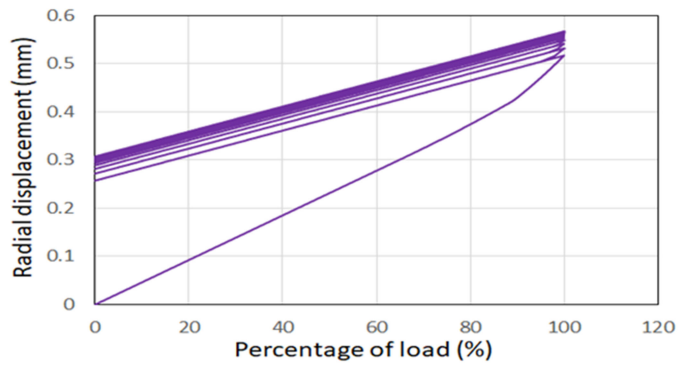


Fig. 8. Calculated radial displacement in the mid-plane of the coil 4 with the new design during 195 cycles of full-field 60T pulses.

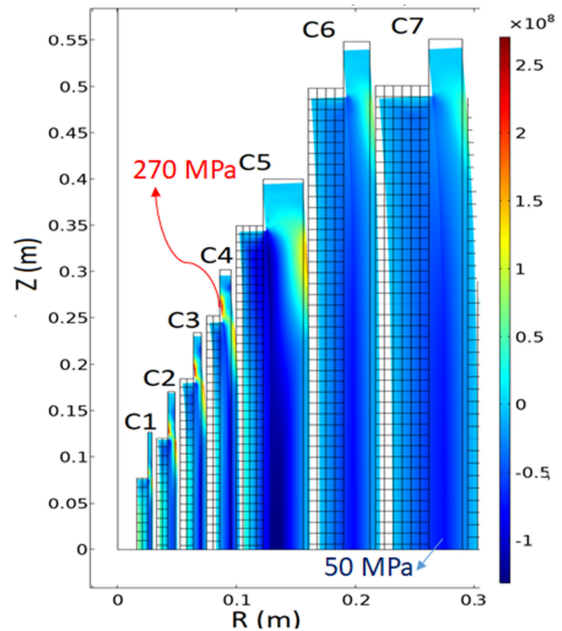


Fig. 9. Axial stress distribution for a quarter of cross-section of the magnet at 60T field (old design).

load condition, the simulated radial displacement for the old design reaches 1.8 mm, quite close the actual value in Fig. 6. With lower stress, displacement of the new coil 4 is much lower, about 0.31 mm, after the same number of full-field pulses. For the new design, deformation is progressed at a much slower pace compared to the old design. This suggested the new design would significantly improve the magnet life-time.

As mentioned before, it is important to check the capability to handle the axial load for the new design with Zylon composite. Figs. 9 and 10 illustrate the axial stress in a quarter of the cross-section of the magnet with the old and new designs, respectively. Generally, most of the cross-section of reinforcing layers experience axial compressive stress due to the axial compressive Lorentz forces on the windings. However, in the region near the coils ends, reinforcing layers undergo tensile stresses caused by the large gradient of the hoop load. Ni-40 shells take most of those axial compressive and tensile stresses. Results in Figs. 9 and 10 indicate that adding Zylon increases both compressive and tensile stresses in coil 3, 4, and 7. However, the highest

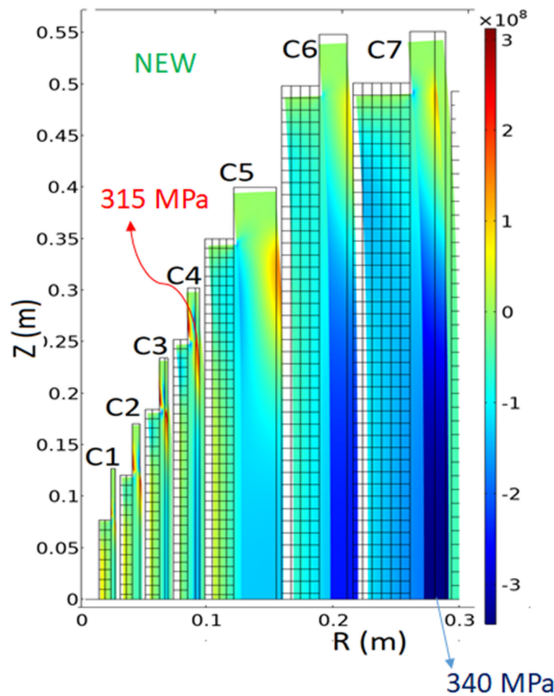


Fig. 10. Axial stress distribution for a quarter of cross-section of the magnet at 60T field (new design).

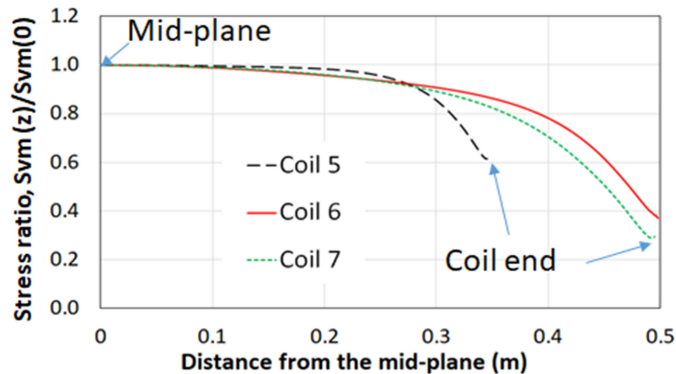


Fig. 11. Stress ratio, $S_{vm}(z)/S_{vm}(z=0)$ as function of z , the distance from the mid-plane along the coil.

tensile stress of 315 MPa in the Ni40 shell of coil 4 and the highest compressive stress of 340 MPa in Ni40 shell of coil 7 are well under the limit of Ni40 alloy material. Therefore, the proposed amount of added Zylon fiber would not be a concern for the coils to handle the axial stresses.

Table I indicates that coils 5 to 7 need quite a large amount of AL60 conductor which commonly has surface inclusions [10], [13], [14]. Depending on their size, inclusions can considerably decrease the fatigue lifetime of the conductors [14]. It is very challenging to produce long-length AL60 wire for these coils without inclusions. So, inclusions of reasonable sizes could be acceptable at the low stress regions near the coil ends. Fig. 11 plots the von Mises stress ration, $S_{vm}(z)/S_{vm}(z=0)$ for coils 5, 6 and 7 as functions of z , the distance from the mid-plane. The stress at the end of those coils is significantly lower than

that of the mid-plane. For example, the stress at the end of coil 7 is about 30% of the stress at its mid-plane. The plots in Fig. 11 help us to qualify the size and the location to accept inclusions in conductors used for these coils.

III. CONCLUSION REMARKS

With unique features, 60TCW magnet at NHMFL - Los Alamos National Laboratory is one of the most favorite magnets for many user experiments. It usually takes 5 to 6 years to produce the materials and rebuild all the magnet coils. After the second failure in 2014, coils 3, 4 and 7 were required to be rebuilt. However, the present design of these coils is not optimal since the stress level in these coils is quite higher than that of the others. Replacing a suitable amount of the Ni40 shells of these coils with high-tensile strength Zylon fiber composite can significantly reduce the hoop stress in those coils to a desired level without losing the ability of these Ni40 shells to handle the axial stresses. So we believe the design will considerably improve the magnet life-time.

It is challenging to produce defect-free, long continuous lengths of AL60 wires for large coils 5 to 7. Fortunately, the stresses near the ends of these coils are considerably lower than in the mid-plane. Thus, inclusions of reasonable sizes can be accepted for the low stress regions near the ends of the coils.

REFERENCES

- [1] G. S. Boebinger, A. H. Lacerda, H. J. Schneider-Muntau, and N. Sullivan, "The national high magnetic field laboratory's pulsed magnetic field facility in Los Alamos," *Physica B, Condens. Matter*, vol. 294-295, 2001, Art. no. 512.
- [2] S. A. Crooker *et al.*, "Optical spectroscopy of magnetic 2D electron gases at the Los Alamos pulsed magnetic field facility," *Physica B, Condens. Matter*, vol. 298, 2001, Art. no. 369.
- [3] L. J. Campbell, H. J. Boenig, D. G. Rickel, J. B. Schillig, J. R. Sims, and H. J. Schneider-Muntau, "Status of the NHMFL 60 tesla quasi-continuous magnet," *IEEE Trans. Magn.*, vol. 32, no. 4, pp. 2454-2457, Jul. 1996.
- [4] J. Schillig, "Operating experience of the United States' National High Magnetic Field Laboratory 60 T long pulse magnet," *IEEE Trans. Appl. Supercond.*, vol. 10, no. 1, pp. 526-529, Mar. 2000.
- [5] J. R. Sims *et al.*, "The U.S. NHMFL 60 T long pulse magnet," *IEEE Trans. Appl. Supercond.*, vol. 12, no. 1, pp. 480-483, Mar. 2002.
- [6] J. R. Sims *et al.*, "The US-NHMFL 60 T long pulse magnet failure," *IEEE Trans. Appl. Supercond.*, vol. 12, no. 1, pp. 480-483, Mar. 2002.
- [7] E. O. Hall and S. H. Algie, "The sigma phase," *Metallurgical Rev.*, vol. 11, pp. 61-73, 1966.
- [8] C. A. Swenson *et al.*, "Pulse magnet development program at NHMFL," *IEEE Trans. Appl. Supercond.*, vol. 14, no. 2, pp. 1233-1236, Jun. 2004.
- [9] D. N. Nguyen, J. Michel, and C. H. Mielke, "Status and development of pulsed magnets at the NHMFL pulsed field facility," *IEEE Trans. Appl. Supercond.*, vol. 26, no. 4, 2016, Art. no. 4300905.
- [10] T. Adkins *et al.*, "60 T pulsed coil design and manufacturing facility," in *Proc. 25th Int. Conf. Magn. Technol.*, Aug. 2017.
- [11] K. Han, R. Goddard, R. Niu, Y. Xin, and V. Toplosky, "Characterization of nitronic-40 stainless steel shells," *IEEE Trans. Appl. Supercond.*, vol. 31, no. 5, 2021, Art. no. 7800105.
- [12] R. P. Walsh and C. A. Swenson, "Mechanical properties of zylon/epoxy composite at 295K and 77 K," *IEEE Trans. Appl. Supercond.*, vol. 16, no. 2, pp. 1761-1764, Jun. 2006.
- [13] K. Han, R. Niu, J. Lu, and V. Toplosky, "High strength conductors and structural materials for high field magnets," *MRS Adv.*, vol. 1, 2016, Art. no. 1233.
- [14] J. Lu, T. Adkins, I. Dixon, D. Nguyen, and K. Han, "Nondestructive testing of high strength conductors for high field pulsed magnets," *IEEE Trans. Appl. Supercond.*, vol. 30, no. 4, Jun. 2020, Art. no. 6900405.